molecular pharmaceutics

BRIEF ARTICLE

pubs.acs.org/molecularpharmaceutics

A Tumor-Environment-Responsive Nanocarrier That Evolves Its Surface Properties upon Sensing Matrix Metalloproteinase-2 and Initiates Agglomeration to Enhance T_2 Relaxivity for Magnetic Resonance Imaging

Sachiko Matsumura,[*,†,‡] Ichio Aoki,[§] Tsuneo Saga,[§] and Kiyotaka Shiba[†]

[†]Cancer Institute, Japanese Foundation for Cancer Research, Ariake, Koto-ku, Tokyo 135-8550, Japan,
[‡]PRESTO, Japan Science and Technology Agency, Honcho, Kawaguchi, Saitama 332-0012, Japan, and
[§]Molecular Imaging Center, National Institute of Radiological Sciences, Anagawa, Inage-ku, Chiba 263-8555, Japan

Supporting Information

ABSTRACT: We designed and synthesized a modified ferritin as a tumor-environment-responsive nanocarrier. We found that this nanocarrier could evolve its surface properties upon sensing a tumor-associated protease, matrix metalloproteinase-2 (MMP-2), which initiated agglomeration, resulting in the enhancement of T_2 relaxivity for magnetic resonance imaging (MRI). The designed ferritin contained a triad of modifiers composed of (i) a "sensing" segment (substrate peptide of MMP-2), (ii) "hydrophobic" segments and (iii) a "hydrophilic" segment of polyethylene glycol (PEG). The hydrophilic segment ensured the particles' monodispersibility in aqueous conditions. In the presence of MMP-2 activity, the "sensing" segment was cleaved by the enzyme and its submerged "hydrophobic" segments were exposed on the surface, resulting in the initiation of aggregation. Because ferritin contains ferrihydrite in its inner space, this multimerization resulted in the enhancement of T_2 relaxivity, suggesting that this nanocarrier may be useful as a contrast agent in MRI.

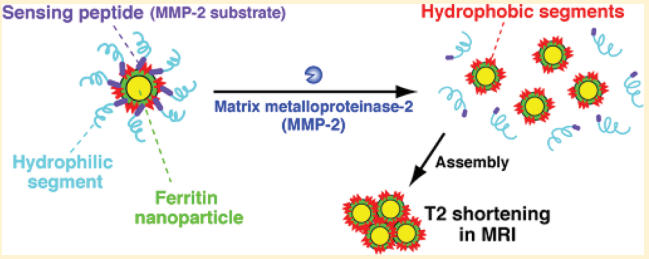

KEYWORDS: assembly, ferritin, magnetic resonance imaging, matrix metalloproteinases, protein nanoparticles, tumor

INTRODUCTION

One of the main goals of nanomedicine is to create a nanocarrier that can efficiently and specifically deliver therapeutic agents to desired target sites in the body. To enable efficient and specific delivery, the nanocarrier needs to have the ability to evolve its properties, such as its size and surface character, by adapting to the surrounding environment. Examples of environment-responsive nanocarriers[1−3] include a recent report by Bae et al.[3] in which the polymer coating is detached from a nanoparticle in a target site, leading to exposure of the TAT peptide on the particle and allowing it to penetrate its target cells.

Tumors develop unique microenvironments, such as slightly acidic pH and higher expression of certain enzymes.[2−5] Although cells in a solid tumor are heterogeneous, which is one of the reasons why the efficacy of therapeutic targeting to tumor cells is restricted, the microenvironments surrounding the tumor cells often share common characteristics.[4,5] Matrix metalloproteinases (MMPs) are engaged in the degradation of extracellular matrices and are tightly associated with malignant processes of tumors, including metastasis and angiogenesis. In particular, MMP-2 has been identified as one of the key MMPs. MMP-2 belongs to a category of type IV collagenases and plays a critical role in the degradation of basement membranes. Enhanced expression of MMP-2 has been reported in many types of human tumors,[6] and therefore, augmented MMP-2 activity can be used as a common signal for tumor-specific microenvironments for prodrugs,[7] drug carriers,[8] and imaging agents.[9,10]

Recently, superparamagnetic nanoparticles that can assemble by responding to MMP-2 activity and can consequently enhance the contrast in magnetic resonance imaging (MRI) have been reported.[11] The selective assembly of nanocarriers in tumor sites has many potential clinical benefits, including the ability to induce a high local concentration of loaded agents in a specific area. In addition, the enlarged form of these assembled nanocarriers can provide other advantages, such as prolongation of the retention time of the agents or signal alternation in MRI.[11−13]

Hence, our goal is to make a nanocarrier that can assemble into larger molecules at tumor sites by responding to the environment specific to a tumor. For this purpose, we focused on MMP-2 as a trigger for the assembly and used a ferritin particle as a nanoparticle vehicle. Ferritin is an iron-storage protein whose structures are well conserved across species. This protein has a

Received: April 15, 2011
Accepted: September 7, 2011
Revised: August 31, 2011
Published: September 07, 2011

dx.doi.org/10.1021/mp2001999 | *Mol. Pharmaceutics* 2011, 8, 1970–1974

spherical hollow structure with an external diameter of 12 nm and an internal diameter of 8 nm and is composed of 24 subunits. In the core inner space, a variety of inorganic materials (besides iron oxide) or small organic molecules can be loaded.[14−16] In addition, the ferritin particle is an excellent vehicle for the multivalent display of peptides on its surface, and prominent improvement in the binding ability of a peptide aptamer, or binder, has been reported when the peptide was displayed on the ferritin surface.[17] These features make ferritin attractive in nanomedical applications.[18,19] Indeed, ferritin has been proposed as a vehicle for drug delivery[20,21] and as a contrast agent in MRI.[13,22,23] Recent reports have shown that the aggregation of ferritin can alter MRI relaxivity.[13,24,25] In this paper, we designed and synthesized a modified ferritin that aggregated upon sensing the activity of MMP-2.

EXPERIMENTAL SECTION

Synthesis of Fer-PPD. The peptide (FAM-Lys-Pro-Leu-Gly-Leu-Ala-Gly-Ahx-Ahx-Ahx-Cys-NH_2, FAM: 5(6)-carboxyfluorescein, Ahx: 6-aminohexanoic acid) was synthesized using the standard Fmoc solid-phase method, purified using reverse-phase HPLC, and identified by MALDI-TOF MS. The peptide was dimerized through the disulfide bond by air oxidation. The side chain of a Lys residue of the peptide was reacted with an *N*-hydroxysuccinimide (NHS) ester of a PEG derivative (average molecular weight: 5 kDa, SUNBRIGHT ME-050AS, NOF, Tokyo), followed by purification with size exclusion chromatography (Sephadex G-50). The disulfide bond in the dimer was reduced with tris[2-carboxyethyl] phosphine hydrochloride (TCEP·HCl), followed by size exclusion chromatography. The obtained peptide−PEG conjugate was coupled with horse spleen ferritin (Sigma Aldrich, St. Louis) using succinimidyl-4-[*N*-maleimidomethyl]cyclohexane-1-carboxy-[6-amidocaproate] (LC-SMCC, Thermo Scientific Pierce, Waltham). Next, cystamine was coupled to this conjugate using 1-ethyl-3-[3-dimethylaminopropyl]carbodiimide hydrochloride (EDC·HCl). Doxorubicin hydrochloride was combined with succinic anhydride, and the obtained derivative was added to the modified ferritin with EDC·HCl and sulfo-NHS (Thermo Scientific Pierce, Waltham). After each reaction of ferritin with the reagents above, ultrafiltration and dialysis were thoroughly carried out to remove excess reagents. Thus, we prepared the ferritin modified with peptide−PEG conjugates and doxorubicin. The concentration of the ferritin was determined using a DC protein assay (Bio-Rad). The number of the peptide−PEG conjugates introduced onto one particle of Fer-PPD was estimated to be 9−14 by the absorption band of FAM at 494 nm using the modified ferritin having only peptide−PEG conjugates (Fer-PP). The coupling with doxorubicin was confirmed by the broadening of the absorption band with a rise of absorption at 550−600 nm, accompanied by a visual change from yellowish green to reddish brown. Peptide cleavage between Gly and Leu by MMP-2 was analyzed by reverse-phase HPLC and MALDI-TOF MS. After treatment of the substrate peptide with MMP-2, the cleaved peptide fragment (FAM-Lys-Pro-Leu-Gly-OH) was detected: m/z calcd 772.8 $[M + H]^+$, found 771.8. Amounts of the cleaved peptide−PEG fragment were estimated by the elution peak area on HPLC (Cosmosil C18-AR-II column, detected at 440 nm, corresponding to the absorption band of FAM) using a standard curve.

Dynamic Light Scattering. The hydrodynamic diameter of Fer-PPD was estimated by dynamic light scattering (DLS) measurements using a Zetasizer Nano ZS (Malvern). The aggregate formation was evaluated by monitoring the z-average diameter. Fer-PPD was incubated in 40 mM Tris·HCl, 150 mM NaCl, 10 mM $CaCl_2$, pH 7.4 at 37 °C.

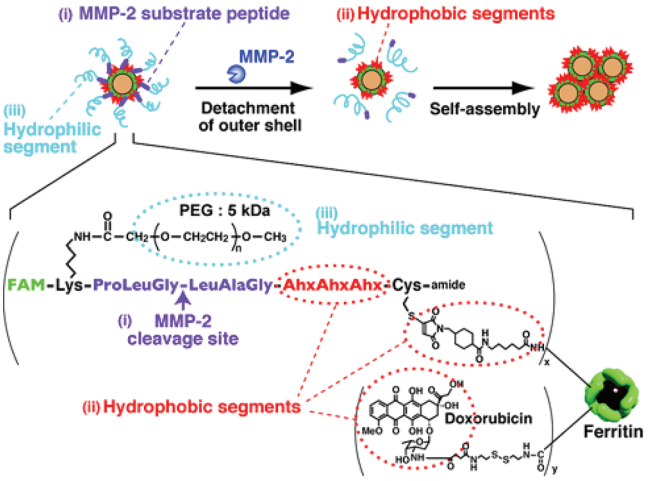

Figure 1. Design of the modified ferritin, Fer-PPD, and a schematic illustration of the assembly of ferritin.

Transmission Electron Microscopy. The sample solution was absorbed onto a collodion-coated copper EM grid (200 mesh). After washing with water, the samples on the grid were negatively stained with aqueous uranyl acetate (2% w/v). The micrographs were obtained using a Hitachi H-7500 electron microscope operating at 80 or 100 kV.

MRI Measurements and Data Analysis. Samples were put into a 96-well tube (INA OPTIKA, Osaka, Japan) and imaged at room temperature (23 °C). The MRI acquisitions were performed in a 7.0 T, 40 cm bore magnet (Kobelco and Jastec, Kobe, Japan) interfaced to a Bruker Avance-I console (Bruker Biospin, Ettlingen, Germany). A 35 mm diameter birdcage coil (Rapid Biomedical, Limper, Germany) was used for measurement of the samples. 2D single-slice multiecho imaging was performed to generate T_2 maps with the following parameters: pulse repetition time (TR) = 3,000 ms, echo time (TE) = 10 to 200 ms, number of echoes = 20, matrix size = 256 × 256, slice orientation = horizontal, field of view = 25.6 × 40.0 mm, slice thickness = 1 mm, and number of acquisitions = 2. For these images, the nominal voxel resolution was 100 μm × 156 μm × 1000 μm. The total acquisition time for multiecho imaging was 25.6 min. Quantitative T_2 maps were calculated by nonlinear least-squares fitting using multiecho imaging.

RESULTS

The designed ferritin had tripartite modifiers including (i) a "sensing" segment, (ii) "hydrophobic" segments and (iii) a "hydrophilic" segment (Figure 1). The "sensing" segment is a hexapeptide (Pro-Leu-Gly-Leu-Ala-Gly) that is known to be a substrate peptide for MMP-2 and thus can be cleaved between Gly and Leu in the presence of the enzyme.[9] Three moieties contributed to the "hydrophobic" segments. One of these moieties is the hydrophobic 6-aminohexanoic acid (Ahx-Ahx-Ahx) that was linked to the C-terminus of the "sensing" segment. The second hydrophobic segment is a cross-linker, succinimidyl-4-[*N*-maleimidomethyl]cyclohexane-1-carboxy-[6-amidocaproate], which links the Cys at the C-terminus of Ahx-Ahx-Ahx with the ferritin surface. The third hydrophobic segment is doxorubicin, which was linked onto the ferritin surface using cystamine as a

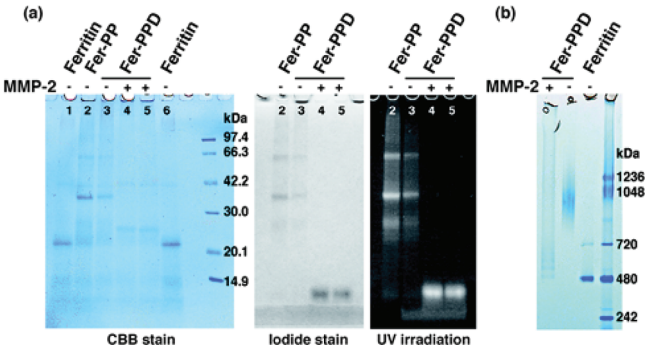

Figure 2. Analysis of Fer-PPD by SDS−PAGE (a) and native PAGE (b) in the presence and absence of MMP-2. Fer-PP is ferritin modified with peptide−PEG conjugates. The same amount of Fer-PPD was loaded onto the two lanes in (b).

linker. We used 5 kDa polyethylene glycol (PEG) for the "hydrophilic" segment, which was linked to the side chain of Lys at the N-terminus of the "sensing" segment. Carboxyfluorescein (FAM) was conjugated as a tracer at this Lys residue. Overall, the designed ferritin, which we named Fer-PPD, is covered by a hydrophilic PEG moiety, which can be removed by MMP-2 cleavage at its substrate peptide. After the ablation, the ferritin exposes its hydrophobic surface, composed of the three moieties, and initiates to form aggregates by virtue of hydrophobic interactions. Fer-PPD was synthesized by chemical modification of commercial horse spleen ferritin. The number of the peptide−PEG conjugates introduced onto one particle of Fer-PPD was estimated to be 9−14 by the absorption band of FAM at 494 nm using a modified ferritin that had only peptide−PEG conjugates (Fer-PP).

Sodium dodecyl sulfate−polyacrylamide gel electrophoresis (SDS−PAGE) analysis of Fer-PPD followed by CBB staining showed two bands whose apparent molecular weights were approximately 40 and 60 kDa (Figure 2a). The broad bands at approximately 20 kDa likely included unmodified ferritin monomers and ferritin monomers that were modified with small molecules, such as cross-linkers and doxorubicin. The two bands at 40 and 60 kDa corresponded to the ferritin monomers modified with one and two peptide−PEG segments, respectively. These bands were stained by iodide, which stains PEG molecules,[26] and yielded fluorescence from FAM by UV irradiation. After incubating Fer-PPD with MMP-2, these two bands disappeared. A new band that had an apparent molecular weight of <14 kDa was detected by iodide staining and UV irradiation but was not detected by CBB staining, which indicated that the new band was the cleaved peptide−PEG segment. Cleavage between Gly and Leu in the peptide segment by MMP-2 was confirmed using HPLC and TOF MS. Native PAGE analysis of Fer-PPD showed a broad band at masses ranging from 720 to 1,200 kDa but not near 480 kDa, which would correspond to the mass of unmodified ferritin (Figure 2b). This result indicated that there were apparently no Fer-PPD particles without peptide−PEG segments. After the MMP-2 treatment, several bands were visible between 480 and 720 kDa, along with band(s) tailing from the gel top, which was just slightly stained. These bands likely represent ferritin particles that had lost PEG segments and therefore started to form multimers.

The aggregation properties of Fer-PPD were evaluated using dynamic light scattering (DLS). The hydrodynamic diameter of

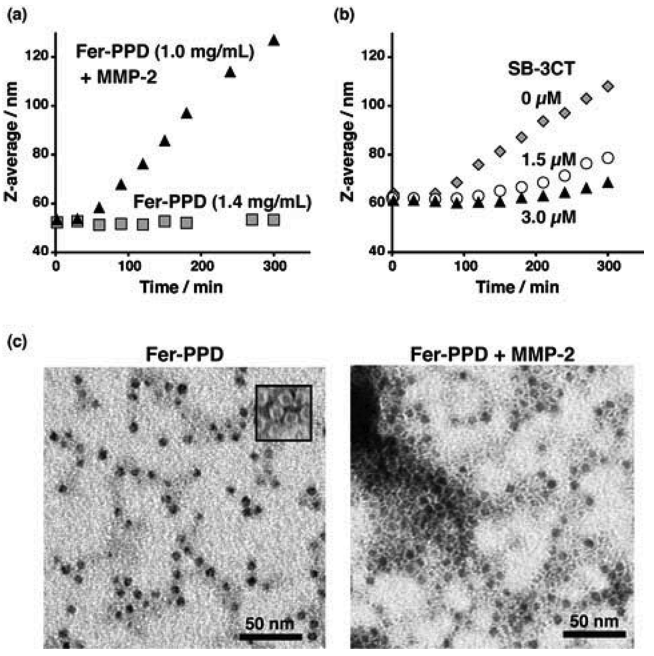

Figure 3. Change of *z*-average over time in the presence and absence of MMP-2. (a) 1.0 mg/mL Fer-PPD and 75 nM MMP-2 (triangle) or 1.4 mg/mL Fer-PPD (square) were incubated in 40 mM Tris·HCl, 150 mM NaCl, 10 mM $CaCl_2$, pH 7.4, at 37 °C. (b) The inhibition of the size change by the addition of 0 (diamond), 1.5 (circle), and 3.0 μM (triangle) MMP-2 inhibitor, SB-3CT, can be seen. 0.75 mg/mL Fer-PPD and 75 nM MMP-2 were incubated in the same conditions as those in (a). (c) This image shows TEM of Fer-PPD before (left) and after (right) addition of MMP-2. Inset: unmodified ferritin. Negatively stained with uranyl acetate.

Fer-PPD in 40 mM Tris·HCl, 150 mM NaCl, and 10 mM $CaCl_2$, and at pH 7.4 and 37 °C was calculated to be 25.8 (±1.4) nm, which is larger than unmodified ferritin (17.1 (±0.8) nm) (Figures S1 and S2 in the Supporting Information). Upon addition of MMP-2, the *z*-average diameter of Fer-PPD increased in a time-dependent manner (Figure 3a). Under the same conditions, we confirmed that 80−90% of the substrate peptide was cleaved within 30 min (Figure S3 in the Supporting Information). The size increase in DLS was suppressed by the addition of an MMP-2 inhibitor, SB-3CT (Figure 3b). These results supported our design in which the detachment of the hydrophilic PEG from the ferritin surface by the cleavage of the substrate peptide by MMP-2 leads to the exposure of the hydrophobic segments on the surface of ferritin, initiating their aggregation.

Transmission electron microscopy (TEM) images further supported the above conclusion. Uranyl acetate stain clearly profiled the particulate structure of unmodified ferritin (inset in Figure 3c); however, the outline of Fer-PPD was not well-defined (Figure 3c). After treatment with MMP-2, the outline of Fer-PPD was distinctly observed to be that of unmodified ferritin (Figure 3c), indicating that the PEG shell surrounding the ferritin particle was removed by MMP-2. Concomitantly, many agglomerates were found with numerous assembled ferritin particles. Ferritin itself was not cleaved by MMP-2 during the period of experiment, as shown by the fact that no broken or degraded forms of the protein were observed in TEM, native PAGE, or SDS−PAGE after treatment with MMP-2.

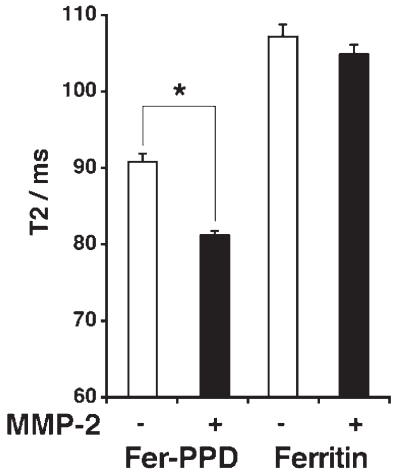

Figure 4. T_2 of Fer-PPD and unmodified ferritin in the presence (black bars) and absence (white bars) of MMP-2. Before T_2 measurement, Fer-PPD and unmodified ferritin (1.0 mg/mL) were incubated with MMP-2 (0 or 21 nM) in the buffer at 37 °C for 24 h. *$P < 0.001$.

The assembly of ferritin particles is expected to result in the reduction of the transverse relaxation times (T_2),[13,24,25] and therefore, T_2 of Fer-PPD in the buffer solution (40 mM Tris·HCl, 150 mM NaCl, 10 mM $CaCl_2$, pH 7.4) was quantitatively evaluated. T_2 of Fer-PPD time-dependently decreased in the presence of MMP-2, but not in the absence of MMP-2 (data not shown). Incubation of Fer-PPD with MMP-2 for 24 h led to an 11% decrease in the T_2 compared to the incubation without MMP-2 (Figure 4, Table S1 in the Supporting Information). The effect of MMP-2 on T_2 at the concentration used in this experiment was negligible (Figure S4 in the Supporting Information), indeed unmodified ferritin showed negligible change in T_2 after incubation with MMP-2. Considering the aggregation properties of Fer-PPD shown in the above experiments, it was concluded that the T_2 shortening was derived from the aggregation of Fer-PPD that was initiated by the detachment of the peptide−PEG segments by MMP-2.

DISCUSSION

As a natural protein in the body, ferritin is one of the most promising carriers for MRI contrast agents. However, native ferritin is a poor MRI contrast agent because its core is not usually fully filled (approximately one-half of the maximum).[27] To resolve this drawback, a reconstituted "magnetoferritin" has been proposed,[23,28,29] wherein the particles are comparable in relaxivity to the existent superparamagnetic iron oxide contrast agents.[23,29] The ferritin particle is very small (approximately 12 nm in a diameter) and is rapidly excreted into the urinary bladder after systemic injection. The assembly of ferritin particles at the tumor site has the potential to prolong the retention and enhance the signal in MRI. Our designed Fer-PPD has the ability to initiate this assembly by sensing the microenvironment of a tumor. The surface of Fer-PPD is ornamented with PEG, retaining dispersibility and avoiding trapping by reticuloendothelial cells.[30] When Fer-PPD reaches the tumor site, it senses the microenvironment of the tumor due to the augmented activity of MMP-2, and the PEG moieties on the surface are detached by the breakage in the sensing segment. The resulting Fer-PPD exposes its sheathed hydrophobic surface, which initiates aggregation of ferritin at the tumor site. The aggregation leads to the shortening of T_2 and susceptibility effects. Therefore, Fer-PPD has the potential to reinforce the contrast in MRI for detecting tumors in the body. Introducing a tumor-specific ligand onto the ferritin surface would be effective in concentrating ferritin particles at the tumor site.[31,32]

Although the T_2 shortening effect induced by the aggregation was clear (11% shorter than unaggregated one), it was not drastic. Furthermore, the aggregation would be suppressed *in vivo* because there are many molecules in physiological fluids, which potentially interact with the modified ferritin to interfere with their aggregation. To improve the aggregation to achieve better contrast, modulation of the hydrophobic segments or the introduction of other assembling motifs[33] might enhance molecular assembly. In addition, congregating ferritin close to each other (e.g., on the order of 100 nm spacing) in or out of cells or on extracellular matrixes using a targeting ligand would be effective to enhance the relaxivity.[24]

CONCLUSION

We demonstrated that the aggregation of ferritin particles, initiated by the action of a tumor-associated protease, MMP-2, led to T_2 shortening in MRI. The ferritin particle was chemically modified with a substrate peptide of MMP-2, three hydrophobic segments and a hydrophilic polymer (PEG). Aggregation of the modified ferritin was clearly demonstrated *in vitro* in this study. Considering the advantages of using the ferritin particle, such as the particle being a natural protein in the body, the inclusion ability of a variety of molecules, and the ease of chemical and genetic modification, ferritin particles have great potential as nanocarriers.

ASSOCIATED CONTENT

Supporting Information. Figures S1−4 and Table S1. This material is available free of charge via the Internet at http://pubs.acs.org.

AUTHOR INFORMATION

Corresponding Author

*Cancer Institute, Japanese Foundation for Cancer Research, 3-8-31 Ariake, Koto-ku, Tokyo 135-8550, Japan. Phone: +81-3-3570-0489. Fax: +81-3-3570-0461. E-mail: sachiko.matsumura@jfcr.or.jp.

ACKNOWLEDGMENT

We thank Dr. Hisakazu Mihara and Dr. Tsuyoshi Takahashi for MALDI-TOF MS and TEM experiments, Mr. Shigeyoshi Saito for MRI operation and Dr. Mitsuru Koizumi and Ms. Tamiko Minamisawa for helpful discussion. This work was supported by JST PRESTO program.

REFERENCES

(1) Gullotti, E.; Yeo, Y. Extracellularly activated nanocarriers: a new paradigm of tumor targeted drug delivery. *Mol. Pharmaceutics* **2009**, *6*, 1041–1051.

(2) Romberg, B.; Hennink, W. E.; Storm, G. Sheddable coatings for long-circulating nanoparticles. *Pharm. Res.* **2008**, *25*, 55–71.

(3) Lee, E. S.; Gao, Z.; Bae, Y. H. Recent progress in tumor pH targeting nanotechnology. *J. Controlled Release* **2008**, *132*, 164–170.

(4) Rademakers, S. E.; Span, P. N.; Kaanders, J. H.; Sweep, F. C.; van der Kogel, A. J.; Bussink, J. Molecular aspects of tumour hypoxia. *Mol. Oncol.* **2008**, *2*, 41–53.

(5) Fukumura, D.; Jain, R. K. Tumor microvasculature and microenvironment: targets for anti-angiogenesis and normalization. *Microvasc. Res.* **2007**, *74*, 72–84.

(6) Turpeenniemi-Hujanen, T. Gelatinases (MMP-2 and −9) and their natural inhibitors as prognostic indicators in solid cancers. *Biochimie* **2005**, *87*, 287–297.

(7) Atkinson, J. M.; Siller, C. S.; Gill, J. H. Tumour endoproteases: the cutting edge of cancer drug delivery? *Br. J. Pharmacol.* **2008**, *153*, 1344–1352.

(8) Terada, T.; Iwai, M.; Kawakami, S.; Yamashita, F.; Hashida, M. Novel PEG-matrix metalloproteinase-2 cleavable peptide-lipid containing galactosylated liposomes for hepatocellular carcinoma-selective targeting. *J. Controlled Release* **2006**, *111*, 333–342.

(9) Jiang, T.; Olson, E. S.; Nguyen, Q. T.; Roy, M.; Jennings, P. A.; Tsien, R. Y. Tumor imaging by means of proteolytic activation of cell-penetrating peptides. *Proc. Natl. Acad. Sci. U.S.A.* **2004**, *101*, 17867–17872.

(10) Bremer, C.; Tung, C. H.; Weissleder, R. In vivo molecular target assessment of matrix metalloproteinase inhibition. *Nat. Med.* **2001**, *7*, 743–748.

(11) Harris, T. J.; von Maltzahn, G.; Derfus, A. M.; Ruoslahti, E.; Bhatia, S. N. Proteolytic actuation of nanoparticle self-assembly. *Angew. Chem., Int. Ed.* **2006**, *45*, 3161–3165.

(12) Perez, J. M.; Josephson, L.; O'Loughlin, T.; Hogemann, D.; Weissleder, R. Magnetic relaxation switches capable of sensing molecular interactions. *Nat. Biotechnol.* **2002**, *20*, 816–820.

(13) Shapiro, M. G.; Szablowski, J. O.; Langer, R.; Jasanoff, A. Protein nanoparticles engineered to sense kinase activity in MRI. *J. Am. Chem. Soc.* **2009**, *131*, 2484–2486.

(14) Yamashita, I.; Iwahori, K.; Kumagai, S. Ferritin in the field of nanodevices. *Biochim. Biophys. Acta* **2010**, *1800*, 846–857.

(15) Abe, S.; Hirata, K.; Ueno, T.; Morino, K.; Shimizu, N.; Yamamoto, M.; Takata, M.; Yashima, E.; Watanabe, Y. Polymerization of phenylacetylene by rhodium complexes within a discrete space of apoferritin. *J. Am. Chem. Soc.* **2009**, *131*, 6958–6960.

(16) Uchida, M.; Kang, S.; Reichhardt, C.; Harlen, K.; Douglas, T. The ferritin superfamily: Supramolecular templates for materials synthesis. *Biochim. Biophys. Acta* **2010**, *1800*, 834–845.

(17) Sano, K.; Ajima, K.; Iwahori, K.; Yudasaka, M.; Iijima, S.; Yamashita, I.; Shiba, K. Endowing a ferritin-like cage protein with high affinity and selectivity for certain inorganic materials. *Small* **2005**, *1*, 826–832.

(18) Maham, A.; Tang, Z.; Wu, H.; Wang, J.; Lin, Y. Protein-based nanomedicine platforms for drug delivery. *Small* **2009**, *5*, 1706–1721.

(19) Cormode, D. P.; Jarzyna, P. A.; Mulder, W. J.; Fayad, Z. A. Modified natural nanoparticles as contrast agents for medical imaging. *Adv. Drug Delivery Rev.* **2010**, *62*, 329–338.

(20) Yan, F.; Zhang, Y.; Yuan, H. K.; Gregas, M. K.; Vo-Dinh, T. Apoferritin protein cages: a novel drug nanocarrier for photodynamic therapy. *Chem. Commun.* **2008**, 4579–4581.

(21) Yang, Z.; Wang, X.; Diao, H.; Zhang, J.; Li, H.; Sun, H.; Guo, Z. Encapsulation of platinum anticancer drugs by apoferritin. *Chem. Commun.* **2007**, 3453–3455.

(22) Aung, W.; Hasegawa, S.; Koshikawa-Yano, M.; Obata, T.; Ikehira, H.; Furukawa, T.; Aoki, I.; Saga, T. Visualization of *in vivo* electroporation-mediated transgene expression in experimental tumors by optical and magnetic resonance imaging. *Gene Ther.* **2009**, *16*, 830–839.

(23) Uchida, M.; Terashima, M.; Cunningham, C. H.; Suzuki, Y.; Willits, D. A.; Willis, A. F.; Yang, P. C.; Tsao, P. S.; McConnell, M. V.; Young, M. J.; Douglas, T. A human ferritin iron oxide nano-composite magnetic resonance contrast agent. *Magn. Reson. Med.* **2008**, *60*, 1073–1081.

(24) Bennett, K. M.; Shapiro, E. M.; Sotak, C. H.; Koretsky, A. P. Controlled aggregation of ferritin to modulate MRI relaxivity. *Biophys. J.* **2008**, *95*, 342–351.

(25) Gossuin, Y.; Gillis, P.; Muller, R. N.; Hocq, A. Relaxation by clustered ferritin: a model for ferritin-induced relaxation *in vivo*. *NMR Biomed.* **2007**, *20*, 749–756.

(26) Sims, G. E.; Snape, T. J. A method for the estimation of polyethylene glycol in plasma protein fractions. *Anal. Biochem.* **1980**, *107*, 60–63.

(27) Chasteen, N. D.; Harrison, P. M. Mineralization in ferritin: an efficient means of iron storage. *J. Struct. Biol.* **1999**, *126*, 182–194.

(28) Meldrum, F. C.; Heywood, B. R.; Mann, S. Magnetoferritin: in vitro synthesis of a novel magnetic protein. *Science* **1992**, *257*, 522–523.

(29) Clavijo Jordan, V.; Caplan, M. R.; Bennett, K. M. Simplified synthesis and relaxometry of magnetoferritin for magnetic resonance imaging. *Magn. Reson. Med.* **2010**, *64*, 1260–1266.

(30) van Vlerken, L. E.; Vyas, T. K.; Amiji, M. M. Poly(ethylene glycol)-modified nanocarriers for tumor-targeted and intracellular delivery. *Pharm. Res.* **2007**, *24*, 1405–1414.

(31) Uchida, M.; Flenniken, M. L.; Allen, M.; Willits, D. A.; Crowley, B. E.; Brumfield, S.; Willis, A. F.; Jackiw, L.; Jutila, M.; Young, M. J.; Douglas, T. Targeting of cancer cells with ferrimagnetic ferritin cage nanoparticles. *J. Am. Chem. Soc.* **2006**, *128*, 16626–16633.

(32) Lin, X.; Xie, J.; Niu, G.; Zhang, F.; Gao, H.; Yang, M.; Quan, Q.; Aronova, M. A.; Zhang, G.; Lee, S.; Leapman, R.; Chen, X. Chimeric ferritin nanocages for multiple function loading and multimodal imaging. *Nano Lett.* **2011**, *11*, 814–819.

(33) Matsui, T.; Matsukawa, N.; Iwahori, K.; Sano, K.; Shiba, K.; Yamashita, I. Realizing a two-dimensional ordered array of ferritin molecules directly on a solid surface utilizing carbonaceous material affinity peptides. *Langmuir* **2007**, *23*, 1615–1618.